energies

MDPI

Article

Analysis of Techno–Economic and Social Impacts of Electric Vehicle Charging Ecosystem in the Distribution Network Integrated with Solar DG and DSTATCOM

Ramesh Bonela [1], Sriparna Roy Ghatak [1], Sarat Chandra Swain [1], Fernando Lopes [2,*], Sharmistha Nandi [1], Surajit Sannigrahi [3] and Parimal Acharjee [4]

[1] School of Electrical Engineering, KIIT Deemed to be University, Bhubaneswar 751024, India; bonelarami@gmail.com (R.B.); sreeparna.ghatak@gmail.com (S.R.G.); scswainfel@kiit.ac.in (S.C.S.); sharmisthanandi38@gmail.com (S.N.)
[2] National Laboratory of Energy and Geology, 1649-038 Lisbon, Portugal
[3] Electrical Engineering Department, National Institute of Technology, Raipur 492010, India; surajit710@yahoo.in
[4] Electrical Engineering Department, National Institute of Technology, Durgapur 713209, India; parimal.acharjee@ee.nitdgp.ac.in
* Correspondence: fernando.lopes@lneg.pt

Abstract: In this work, a comprehensive planning framework for an electric vehicle charging ecosystem (EVCE) is developed, incorporating solar distributed generation (DG) and a distribution static compensator (DSTATCOM), to assess their long-term techno–economic and environmental impacts. The optimal locations and capacities of the EVCE, solar DG, and DSTATCOM are determined using an improved particle swarm optimization algorithm based on the success rate technique. The study aims to maximize the technical, financial, and social benefits while ensuring that all security constraints are met. To assess the financial viability of the proposed model over a 10-year horizon, a detailed economic analysis comprising installation cost, operation, and maintenance cost is conducted. To make the model more realistic, various practical parameters, such as the inflation rate and interest rate, are incorporated during the financial analysis. Additionally, to highlight the societal benefits of the approach, the study quantifies the long-term carbon emissions and the corresponding cost of emissions. The proposed framework is tested on both a 33-bus distribution network and a 108-bus Indian distribution network. Various planning scenarios are explored, with different configurations of the EVCE, solar-based DG, and DSTATCOM, to assist power system planners in selecting the most suitable strategy.

Keywords: distributed generation; distribution network; distribution static compensator; electric vehicle; optimal planning

check for updates

Academic Editors: Massimiliano Coppo and Marina Bertolini

Received: 16 December 2024
Revised: 9 January 2025
Accepted: 13 January 2025
Published: 16 January 2025

Citation: Bonela, R.; Roy Ghatak, S.; Swain, S.C.; Lopes, F.; Nandi, S.; Sannigrahi, S.; Acharjee, P. Analysis of Techno–Economic and Social Impacts of Electric Vehicle Charging Ecosystem in the Distribution Network Integrated with Solar DG and DSTATCOM. *Energies* **2025**, *18*, 363. https://doi.org/10.3390/en18020363

Copyright: © 2025 by the authors. Licensee MDPI, Basel, Switzerland. This article is an open access article distributed under the terms and conditions of the Creative Commons Attribution (CC BY) license (https://creativecommons.org/licenses/by/4.0/).

1. Introduction

Driven by the need for sustainable mobility, reduced greenhouse gas emissions, and energy independence, the swift integration of Electric Vehicles (EVs) is transforming the transportation sector. EVs stand out due to their eco-friendly and cost-effective nature. Unlike traditional vehicles, EVs produce no vehicular emissions, require less maintenance, and significantly reduce the dependence on fossil fuels. These features make them a sustainable and economically viable choice for modern transportation [1]. Despite the numerous advantages of EVs, their widespread adoption is significantly constrained by the inadequate development of a robust EV charging ecosystem (EVCE), creating a major

obstacle for EV users. However, the integration of EVCEs imposes additional demands on the power system, potentially resulting in grid congestion, increased system losses, voltage fluctuations, and breaches of operational constraints [2]. To address these challenges, the development of an efficiently planned EVCE is critical. Suitable EVCEs not only ensure accessibility and convenience for EV users but also play a pivotal role in minimizing grid impacts. An effective EVCE should have a sufficient number of chargers to reduce the waiting time of the users as well as their range anxiety while maintaining the power system constraints [3].

To further accelerate the shift towards greener and more eco-friendly energy alternatives, the planning should incorporate distributed generation (DG) powered by renewable energy sources in the distribution network (DN) [4]. Renewable-based DGs encompassing solar, wind, hydroelectric, and other forms of clean energy contribute significantly to reducing carbon emissions, enhancing energy efficiency, and promoting decentralized energy generation. In this context, the solar DG is an ideal choice for integration into the DN in tropical countries like India, where solar irradiation is abundant [5]. However, the power output of renewable energy sources is highly dependent on factors such as time of day, climatic factors, the surrounding temperature, and solar intensity. This variability presents considerable difficulties for utility companies in integrating large-scale renewable energy into the grid while ensuring adherence to operational constraints [6]. To mitigate these challenges, capacitor banks can be used; however, these come with several drawbacks, including limited harmonic tolerance, overvoltage issues, fixed reactive power compensation, temperature sensitivity, switching transients, limited lifespan, fire hazards, and the use of non-renewable materials, etc., making them unsuitable for long-term solutions [7].

The expansion of existing power systems has been significantly constrained by a variety of economic, environmental, technical, and legal factors. Consequently, with the continuous rise in load demand, power systems worldwide are increasingly compelled to operate their equipment at near-maximum capacity, pushing stability limits [8]. In recent years, power system planners and researchers have grown increasingly concerned about voltage stability issues, recognizing these as a critical factor contributing to power system insecurity, instability, and even voltage collapse [9]. Voltage stability refers to the capability of a power system to maintain bus voltages within acceptable levels despite experiencing either minor or significant disturbances. As system loading increases, the demand for real and reactive power rises, often leading to a reduction in bus voltages. If this voltage drop exceeds a critical threshold, the system may experience voltage instability [10]. In heavily loaded networks, the challenge of voltage instability can be alleviated, at least partially, through the deployment of shunt-compensating devices such as static VAR compensators (SVCs), which are part of the flexible AC transmission system (FACTS) family. These devices play a crucial role in improving voltage profiles and enhancing system stability [11,12].

In recent times, the distribution static compensator (DSTATCOM) has become a popular choice among power system engineers due to its effectiveness in managing the intermittency of renewable energy sources [13]. The DSTATCOM operates dynamically to manage reactive power. When the voltage falls below the desired level, it injects reactive power into the system. On the other hand, if the voltage exceeds the desired level, it absorbs reactive power to maintain balance. By dynamically stabilizing voltage and improving power quality without relying on extensive energy storage, the DSTATCOM enhances grid stability [14]. This makes it a more sustainable and efficient solution for the long-term integration of renewable-based DG into the grid [15].

Further, there are several challenges associated with DN that demand the focus of power system planning engineers to maintain system stability and reliability. One of the primary technical issues encountered in radial DN is the occurrence of low voltage levels,

a low power factor, and a high R/X ratio [16]. The higher R/X ratio of distribution lines causes considerable power losses and has a major impact on the voltage stability of the system. These technical parameters of the system experience further deterioration when an EVCE is integrated. Therefore, to improve the efficiency of the system incorporating an EVCE, it is crucial to scheme a resilient framework of a DN that considers the renewable-based DG as well as the DSTATCOM [17,18].

Therefore, the planning of an EVCE must incorporate the solar DG and DSTATCOM to ensure a holistic approach to sustainable power system planning and operation [19]. A comprehensive analysis of these integrated components is crucial for achieving an efficient, reliable, and environmentally friendly energy network that meets the growing demands of power systems.

The authors in [20], identified the optimal sites and capacities for an EVCE within a 33-bus DN. Their approach utilized a stochastic power flow analysis to ensure voltage stability throughout the network. The authors aimed to maximize the annual profit gain, the charging convenience of EV users, and the stability of the system. In another paper [21], the researchers optimized the location of the EV charging infrastructure using a modified teaching–learning-based optimization that aimed to improve voltage stability, reduce energy losses, and enhance system reliability. The authors in [22] optimally identified the sites and sizes of the different types of charging stations within a DN. The paper aimed to minimize the number of charging stations and corresponding investment costs. In [23], the study focused on optimizing the size and placement of an EVCE to minimize system losses, voltage profile deterioration, and installation costs. The balance mayfly algorithm was employed to determine the optimal locations of the EVCE. In [24,25], the authors utilized particle swarm optimization (PSO) and grey wolf optimization methods, respectively, to identify suitable locations for charging stations. Their primary objective was to reduce system losses across the DN.

Although the aforementioned studies provide significant insights, they fail to address the incorporation of renewable generation, a critical aspect for ensuring a more sustainable and eco-conscious solution.

A strategy for managing energy in an EV charging infrastructure powered by solar DG and biogas was proposed in [26]. This research carried out a techno–economic evaluation aimed at reducing the costs associated with charging and easing the pressure on the grid due to the high demand for EVs. In [27], a detailed framework for a fast EV charging infrastructure that operates with solar energy and battery storage was presented. The research aimed to optimize the number of chargers and the sizing of the solar power DG while minimizing power losses, voltage deviations, and the associated investment, operational, and maintenance costs. In another study [28], the authors proposed an energy management strategy while determining the optimal site and size of a charging infrastructure incorporating solar-based renewable sources. The objective of the paper was to reduce the strain on the energy network while taking into account the advantages for both the charging station operators and EV users. The literature indicates that previous studies have often integrated renewable energy sources without including reactive power compensating devices, which are crucial for controlling the voltage and stability, and thus managing the intermittency of renewable energy.

A two-phase approach for identifying the best locations for renewable-based DG and capacitor banks was presented in Refs. [29,30] that aimed to minimize overall system losses, reduce voltage fluctuations, and improve the stability of low- and medium-voltage networks. However, problems related to the overvoltage issue, fixed reactive power compensation, temperature sensitivity, and switching transient were not addressed by the previous studies. In this context, the DSTATCOM plays a crucial role in addressing

these challenges. A multi-stage plan for an EV charging station with the presence of a DG and DSTATCOM is presented in [31]. The authors performed the optimal allocation of an EVCE, DG, and DSTATCOM considering the energy loss and EV-user convenience factor. In another study [32], the researchers performed the simultaneous allocation of a DG and DSTATCOM while addressing the impacts of an EV charging infrastructure on the DN. The authors aimed at a reduction in power loss, the enhancement of voltage stability, and improvement of the voltage magnitude while optimizing the sizes of the DG and DSTATCOM. In [33], the authors proposed a planning model that incorporated a DG and DSTATCOM within a reconfigured radial 33-bus and 69-bus distribution network. The authors aimed to minimize the active and reactive power losses and voltage deviation and to improve the reliability of the system using adaptive PSO and a hybrid gray wolf–particle swarm optimization technique. In another paper [34], the authors proposed a power management strategy in order to optimize the active and reactive power flow in a radial DN by integrating DG and multi-shunt compensator-based STATCOM devices. The paper aimed to optimize the power losses of the system as well as the loading margin. Another study [35] considered the optimal placement and sizing of a DSTATCOM in a DN with the aim of reducing the total investment cost and energy loss cost using a sine–cosine optimization algorithm.

Although the previous studies [16–24] have made significant contributions, there is a need for a comprehensive analysis considering technical, economic, and environmental factors that are missing in prior research. These assessments are vital for guaranteeing the financial efficiency and long-term viability of the planning process, while also addressing the challenges associated with EV charging demand and intermittent renewable energy sources.

Soft computing techniques are powerful for solving complex, nonlinear, and uncertain optimization problems [36]. These methods are particularly useful for real-world applications, where traditional approaches may struggle [23]. Among them, PSO stands out due to its simplicity, fast convergence, and versatility. However, PSO can suffer from premature convergence and difficulties in balancing exploration and exploitation. These challenges can be mitigated by improving the parameters of the conventional PSO [16].

To address the research gap identified through the literature review, an effective planning model for an EVCE incorporating renewable-based DG and DSTATCOM needs to be developed, considering all techno–economic and environmental aspects. The innovative aspect of this research lies in developing the planning model of a DN incorporating an EVCE, solar DG, and DSTATCOM considering different technical, financial, and environmental aspects. The optimal location and sizing of the EVCE, solar DG, and DSTATCOM are determined using the improved particle swarm optimization based on success rate (IPSO-SR) algorithm while ensuring that power system security constraints are met [16]. Different techno–economic and social indices are employed to assess the long-term practicability and sustainability of the designed planning model. Further, to evaluate the system's capacity to accommodate a growing number of EVs while maintaining stability and efficiency, the EV penetration level is also quantified. To establish the generality of the study, the current model is verified on both a 33-bus DN [37,38] and a 108-bus Indian urban DN [3,39] over a period of 10 years.

The key contributions of the present work are provided below.

- A robust planning model of radial DN is designed incorporating EVCE, solar DG, and DSTATCOM;
- The study aims to identify the location and size of the EVCE, solar DG and DSTATCOM optimally employing IPSO-SR, with the goal of optimizing both economic performance and social advantages. The optimization process ensures compliance

with system security constraints, including power balance, power flow, voltage, and power factor limits;

- A comprehensive financial assessment is conducted, covering the installation expenses, operational and maintenance costs, energy loss charges, and emission-related costs over an extended period. The analysis also incorporates the interest rate and inflation rate to efficiently model the future cost of the planning;
- Various case studies of different configurations of EVCE, solar DG, and DSTATCOM are conducted to compare key techno–economic factors to help the planning engineers of the power system select the optimal strategy.

2. EV Charging Ecosystem (EVCE), Solar Distributed Generation (DG) and Distribution Static Compensator (DSTATCOM)

An EVCE comprises several essential components that ensure efficient and safe vehicle charging. The power supply unit connects the station to the electrical grid or renewable energy sources, often using transformers to step down a high voltage to suitable levels. The charging unit includes a charge controller, which manages the flow of current and voltage, and connectors or chargers compatible with standards such as level 1, level 2, or level 3. A power conversion system is integral to the station, converting alternating current (AC) from the grid to direct current (DC) for fast charging. In the present work, 10 kW AC slow charging is considered to charge the vehicle. The EVCEs are integrated into the 33-bus and 108-bus DN. Therefore, the total load of the system is considered as a combination of the existing load of the network and the load for EV charging, as follows:

$$\text{Total load} = \text{Existing load of Distribution network} + \text{EVCE load}$$

Distributed generation, or DG, refers to low-rated electric power generators (usually ranging from 1 KW to 50 MW) that may directly supply the load's electrical needs at the distribution site. Photovoltaic, wind, microturbines, small hydro turbines, combined heat and power, and hybrid are the various forms of distributed generation. Smaller generating units, known as DGs, are positioned close to load centers in order to prevent the power system network requirements from being expanded. In the present work, the DG is modelled as a real power solar photovoltaic (PV) source. One of the key advantages of solar PV systems over traditional energy systems is their ability to convert solar energy directly into electricity, bypassing the need for thermal–mechanical processes. In addition to being dependable, it is also eco-friendly, noiseless, and suitable for practically any environment.

A DSTATCOM is a device that connects in parallel with the power system using a voltage source converter and interacts with DN via a transformer. It delivers both inductive and capacitive reactive power support. The primary elements consist of a DC capacitor, an AC filtering system, a transformer, and an inverter unit. These elements work together to regulate voltage and improve power quality by compensating for reactive power in the electrical grid. Compared to traditional reactive power compensation devices, the DSTATCOM has several advantages such as a compact design, minimal noise, and lower harmonic distortion. Due to these benefits, the DSTATCOM is frequently deployed in radial DNs to enhance power quality by tackling various challenges, including voltage sag, instability, ineffective voltage control, and energy losses. In this research, it is represented as a reactive power source for analytical purposes.

3. Objective Function and Constraints

The goal of the present study is to minimize the total planning cost (C_{Total}) in terms of the total investment cost (C_{inv}), cost of energy loss (C_{el}), and the cost of environmental

emissions (C_{ee}) of the EVCE, solar DG, and DSTACOM. The investment cost includes the cost of installation (C_{in}) and the cost of operation and maintenance (C_{om}) for a 10-year planning period.

3.1. Objective Function

$$C_{Total} = (C_{inv} + C_{el} + C_{ee}) \quad (1)$$

$$C_{inv} = (C_{in} + C_{om}) \quad (2)$$

(a) Total cost of installation (C_{in})

The total cost required for installing the EVCE (in_{EVCE}), solar DG (in_{DG}), and DSTATCOM (in_{DST}), in the DN are minimized to ensure economic benefit. The total installation cost can be expressed as follows:

$$C_{in} = in_{EVCE} + in_{DG} + in_{DST} \quad (3)$$

Choosing the best location for a sustainable charging environment is a challenging problem. The objective function of this study incorporates economic, environmental, and technical factors. The EVCE installation cost (in_{EVCE}) is represented in (4), as follows:

$$in_{EVCE}(i) = C_{\text{land}}(i) + C_{\text{lab}}(i) + C_{\text{Cons}}(i) + C_{\text{charger}} \quad (4)$$

where $C_{\text{land}}(i)$ represents the land acquisition cost, $C_{\text{lab}}(i)$ corresponds to labor expenses, and $C_{\text{Cons}}(i)$ denotes the development cost of the ith EVCE. C_{Charger} accounts for the expense of the chargers, which depends on the quantity of chargers and their type. On average, an area of 20 m^2 is the average amount of space needed for EV parking. However, when accounting for the space needed for electrical equipment, maintenance areas, and other facilities, the total area allocated per vehicle at an EVCE is approximately 45 m^2 [40], as follows:

$$C_{\text{land}}(i) = Area(i) \times C_{\text{area}} \quad (5)$$

$$C_{\text{charger}}(i) = N_{slch}(i) \times C_{slch} \quad (6)$$

$$C_{\text{cons}}(i) = Area(i) \times Con_{EVCE} \quad (7)$$

where $Area(i)$ is the area required for ith EVCE, C_{area} is the cost of the area. N_{slch} and C_{slch} are the number of slow chargers and the cost of each slow charger, respectively. Con_{EVCE} indicates the construction cost of each EVCE.

The expression of in_{DG} and in_{DST} are presented below which include the capacity of the solar DG and DSTATCOM and the corresponding cost for installing the devices, as follows:

$$in_{DG}(i) = ic_{DG} \times P_{DG}(i) \times cu \quad (8)$$

$$in_{DST}(i) = ic_{DST} \times Q_{DST}(i) \quad (9)$$

ic_{DG} and ic_{DST} are the cost of installing a solar DG and DSTATCOM, respectively. P_{DG} and Q_{DST} indicate the capacity of the solar DG and DSTATCOM, respectively. cu is the capacity utilization [41].

(b) Total cost of operation and maintenance (C_{om})

Equation (10) illustrates the cost required for operating and maintaining the EVCE, solar DG, and DSTATCOM, which includes the cost of the power purchase, energy costs

for energy supplied by the solar DG and DSTATCOM, and the cost of operating and maintaining the charging station ecosystem for 10 years, as follows:

$$C_{om} = om_{EVCE} + om_{DG} + om_{DST} \tag{10}$$

$$om_{EVCE} = \left(N_{slch}(i) \times R_{slch} \times C_{grid} \times h \times y \times cv\right) + C_{MEV} \tag{11}$$

$$om_{DG} = C_{OMDG} \times P_{DG}(i) \times cu \times y \times cv \tag{12}$$

$$om_{DST} = C_{OMDST} + \left[\left(mQ_{DST}(i)^2 - nQ_{DST}(i)\right) \times h \times y \times cv\right] \tag{13}$$

$$cv = \frac{1 - Pp^y}{1 - Pp} \tag{14}$$

$$Pp = \frac{1 + \left(\frac{Inf}{100}\right)}{1 + \left(\frac{Int}{100}\right)} \tag{15}$$

where R_{slch} is the power rating of the EV chargers and C_{grid} is the cost of electricity. C_{MEV} indicates the maintenance cost of the EVCE. h and y denote the hour and planning years. cv is the current value of the cost of the EVCE, DG, and DSTATCOM. m and n are the cost coefficients associated with the DSTATCOM. Pp is the present price. Inf and Int are the inflation and interest rates, respectively.

(c) Total cost of energy loss (C_{el})

This research focuses on reducing energy loss expenses, a critical factor in enhancing efficiency and preserving resources in power system planning. The cost associated with energy losses is represented as follows:

$$C_{el} = P_{loss} \times C_{grid} \times h \times y \times cv \tag{16}$$

where P_{loss} is the total system power losses.

(d) Total cost of environmental emissions (C_{ee})

Including emissions costs in the objective function is essential for effective power system planning. This method helps decision-makers prioritize sustainability by highlighting strategies that reduce environmental harm, particularly the emissions of pollutants and greenhouse gases. It guides the identification of solutions that contribute to cleaner energy production and a lower carbon footprint, as follows:

$$C_{CO_2} = EF_{grid} \times Pow_{grid} \tag{17}$$

$$C_{ee} = C_{CO_2} \times E_{CO_2} \times h \times y \times \frac{1}{(1+r)^y} \tag{18}$$

where C_{CO_2} indicates the cost of generated CO_2. EF_{grid} is the emissions factor of the grid and E_{CO_2} is the price of emitted CO_2. r denotes the discount rate. All objective functions are scaled between 0 and 1 to ensure comparability [37].

3.2. Constraints

Maintaining equality and inequality constraints within suitable limits is crucial for satisfactory power system operation.

(a) Power balance constraints

The total active and reactive power demand (P_{demand}, Q_{demand}), along with the system's active and reactive power losses (P_{loss}, Q_{loss}), should not exceed the total active and

reactive power generation from the grid (AP_{grid}, RP_{grid}) as well as the DG and DSTATCOM (P_{DG}, Q_{DST}), as shown below:

$$AP_{grid} + P_{DG} = P_{demand} + P_{loss} \quad (19)$$

$$RP_{grid} + Q_{DST} = Q_{demand} + Q_{loss} \quad (20)$$

(b) Power flow constraints

The power transmitted ($P_{flow}{}^{l}$) through each network line (l) must not exceed the maximum threshold (P_{flow}^{max}) to guarantee the secure functioning of the power system, as defined by the following conditions:

$$P_{flow,i}^{\ l} < P_{flow}^{max} \quad (21)$$

(c) Voltage constraints

The bus voltage (V_i) must stay within a defined range, constrained by the minimum (V_{min}) and maximum (V_{max}) limits, as defined in (22), as follows:

$$V_{min} \leq V_i \leq V_{max} \quad (22)$$

(d) Power factor constraints

The power factor should be maintained within the suitable limit during the operation as shown below:

$$\text{Power Factor} \geq 0.9 \quad (23)$$

4. Problem Formulation

In this study, the primary objective is to optimally identify the locations and sizes of EVCE, solar DG, and DSTATCOM while minimizing the overall cost. The optimization process uses the IPSO-SR algorithm, with input parameters such as bus and line data to minimize the total fitness function. The planning horizon spans 10 years. The efficacy of the proposed methodology is demonstrated by testing it on both 33-bus and 108-bus DNs. The system's performance is assessed based on various techno–economic and environmental factors, including improvements in voltage profiles, reductions in power losses, economic benefits, and environmental advantages. The planning was conducted by considering the following aims:

i. Allocation of EVCE, solar DG, and DSTATCOM in the DN;
ii. Minimization of investment costs including installation and operation–maintenance expenses to ensure a cost-effective approach;
iii. Minimization of energy loss to benefit the power system planning engineer;
iv. Minimization of environmental emissions to address societal benefits.

5. Methodology

The present study proposes a robust planning framework of a DN considering an EVCE, solar DG, and DSTATCOM to address the growing EV charging demand and renewable intermittency. The approach underlying the proposed planning model is outlined below.

5.1. Conventional Particle Swarm Optimization (PSO)

PSO is one of the most popular, naturalistic, swarm-based optimization techniques. The basic idea of PSO is that every "particle", or member of the swarm, represents a po-

tential solution; every particle adjusts its position inside the search area and changes its velocity based on its own experience and the experiences of its neighbor flies at each iteration, aiming for a better position for itself as long as it satisfies specific fitness requirements. Each particle adjusts its position based on the best position found by the particle itself (p^{best}) and the best position found by any particle in the swarm (g^{best}).

The particles update the velocity and position based on (24) and (25), as follows:

Velocity update:

$$v_i(t+1) = w.v_i(t) + c_1.r_1.(p^{best} - x_i(t)) + c_2.r_2.(g^{best} - x_i(t)) \quad (24)$$

Position update:

$$x_i(t+1) = x_i(t) + v_i + (t+1) \quad (25)$$

where, v_i $(t + 1)$ is the modified velocity at $(t + 1)$th iteration, v_i is the current velocity of particle i, w is the inertia weight, c_1 and c_2 are cognitive and social learning factors, and r_1 and r_2 are random numbers between 0 and 1. x_i is the current position of the particle at iteration t and x_i $(t + 1)$ denotes the updated position of the particle at the $(t + 1)$th iteration.

Although the conventional PSO algorithm is often employed, its effectiveness may be hampered by its lack of diversity, premature convergence, or the propensity to become trapped in local optima.

5.2. Improved Particle Swarm Optimization Based on Success Rate (IPSO-SR)

To increase the efficiency, and accuracy of the optimization technique, the inertia weight of the conventional technique is modified using a particle's success rate-based adaptive inertia weight scheme [16]. The adaptive inertia weight can be expressed as follows:

$$ns(i) = \begin{cases} 1, \; if \; FF_i^t > FF_{p^{best},i}^{t-1} \\ 0, \; Otherwise \end{cases} \quad (26)$$

$$nsr = \frac{1}{p}\sum_{i=1}^{p} ns(i) \quad (27)$$

$$w(t) = \left(w^u - w^l\right) \times sr + w^l \quad (28)$$

where $ns(i)$ indicates the number of successes of the particle i. FF_i^t, and $FF_{p^{best},i}^{t-1}$ are the fitness function at the current iteration t and previous iteration $t-1$. sr refers to the success rate of the particle and p is the number of particles. w^u and w^l indicate the upper and lower bounds of the weighting factor (w).

The stepwise procedure of the implementation of IPSO-SR for the determination of the optimal location and sizing of the EVCE, solar DG, and DSTATCOM is provided below.

Step 1: Input network information related to line data and bus data. Set the number of EVCE, DG, and DSTATCOM;
Step 2: Set the parameters for population size and maximum iteration counts, parameters of IPSO-SR, i.e., c_1, c_2, the upper and lower boundaries of the decision variable (size and locations of the EVCE, DG, and DSTATCOM), and velocity;
Step 3: Conduct the load flow analysis using BFS in order to identify the base case power losses and voltage profile;
Step 4: Initialize the decision variables by creating random initial particles of locations and sizes of the EVCE, DG, and DSTATCOM;
Step 5: Calculate the objective function using (1)–(18) and check for security constraint violations such as power balance, voltage, power flow, and power factor constraints using (19)–(23). If any particle does not satisfy the operational constraints, reinitialize the particles;

Step 6: Set the personal best and global best solution as p^{best} and g^{best}, respectively;
Step 7: Calculate the adaptive inertia weight using (26)–(28) and update the velocity as well as the position of the particle using (24) and (25);
Step 8: Update the p^{best} and g^{best} according to the error fitness value of the objective function;
Step 9: Check the convergence criteria, i.e., the maximum number of iterations;
Step 10: If the solution reaches convergence, display the results. If not, proceed to Step 5.

6. Results and Discussion

The suggested approach was applied to optimize the location and size of the EVCE, solar DG, and DSTATCOM in a 33-bus system and 108-bus system to validate its efficacy. The 33-bus network comprised 33 nodes and 32 connecting branches. The active and reactive power of the 33-bus system was 3.715 MW and 2.3 MVAr, with a base voltage of 12.66 KV. Furthermore, 33-bus system baseload losses were 202 KW; the minimum voltage in the system was 0.9131 p.u., observed at bus 18. The data related to 33-bus system is provided in Table A1. Similarly, the 108-bus system consisted of 108 nodes and 107 branches; the overall real and reactive power was 12.132 MW and 9.099 MVAr, with a base voltage of 11 KV, respectively. The 108-bus system's baseload losses were 471.85 KW, with the base load's lowest bus voltage of 0.9224 p.u. at bus number 105. The bus data and line data of 108-bus system is provided in Table A2.

The load flow analysis was performed using the backward–forward sweep method. Additionally, the study employed the IPSO-SR to optimally determine the location and capacity of the EVCE, solar DG, and DSTATCOM. To accomplish this, a MATLAB R2020b program, with an Intel Core i5 CPU and RX-560 GPU, 12th generation, was used. Table 1 presents all the economic and environmental input parameters associated with the objective function.

Table 1. Economic and environmental parameters associated with the fitness function.

Parameters	Values	Parameters	Values
$Area$	45 m^2	ic_{DG}	\$1058/kW
C_{area}	\$824.35/m^2	ic_{DST}	\$68.35/kVAr
C_{slch}	\$941	C_{MEV}	3% of in_{EVCE}
Con_{EVCE}	\$129/m^2	C_{OMDG}	3% of ic_{DG}
C_{lab}	\$29/m^2	C_{OMDST}	5% of ic_{DST}
R_{slch}	10 kW	Inf, Int	5%, 10%
C_{grid}	\$0.0705/kWh	h, y	8760 h, 10 years
V_{min}, V_{max}	0.9 p.u., 1.05 p.u.	r	10%
EF_{grid}	910 kg CO_2/MWh	cu	0.20
E_{CO_2}	\$9.76/ton CO_2	m, n	0.0002478, 0.2261

6.1. Case Description

To assist power system planning engineers in choosing the optimal strategy, different case studies of various configurations of DGs and DSTATCOMs were investigated. The case studies are significant because they provide a thorough grasp of several aspects that need to be considered in order to determine the most advantageous and technically feasible option. Each case demands specific input parameters; for instance, certain cases emphasize maximizing renewable energy utilization to manage grid overload, while others focus on enhancing user convenience. By systematically analyzing and comparing the results across

these varied scenarios, power system planners can determine the most effective strategy for integrating an EVCE into the network. This detailed evaluation will help in selecting the best approach and in balancing technical viability with societal advantages.

a. Base Case: In this case, no EVCE, solar DG, or DSTATCOM systems are integrated into the network;
b. Case I: An EVCE is placed within the network;
c. Case II: an EVCE is integrated with a solar-based DG in the test system;
d. Case III: an EVCE is integrated with a DSTATCOM;
e. Case IV: an EVCE is placed in conjunction with a solar-based DG and DSTATCOM-based reactive power compensators.

6.2. Analysis of Results

(a) Results of sitting and sizing of the EVCE, solar DG, and DSTATCOM

In this study, five locations were selected for the EVCE installations, three for the DGs, and three for the DSTATCOMs, with each location hosting a single unit for a 33-bus system. In the 108-bus system, the EVCE setups were designated for seven locations, while five locations were assigned for the DG units and another five for the DSTATCOM systems, with each location accommodating a single unit. Both the placement and sizing of the EVCE installations, DGs, and DSTATCOMs were determined using IPSO-SR optimization to ensure efficient and effective integration into the power system. The optimal location and sizes of the EVCEs, DGs, and DSTATCOMs for both the 33-bus and 108-bus systems are presented in Figures 1–4 for all four planning cases. From the analysis, the total optimal capacity of DG for the 33-bus system was determined to be 415 kW in Case II and 430 kW in Case IV. For the 108-bus system, the total solar DG capacity was found to be 2091 kW in Case II and 2110 kW in Case IV. Similarly, the total size of the DSTATCOM for the 33-bus system was calculated as 435 kVAr in Case III and 450 kVAr in Case IV. In the 108-bus system, the DSTATCOM size was 1800 kVAr in Case III and increased to 1878 kVAr in Case IV.

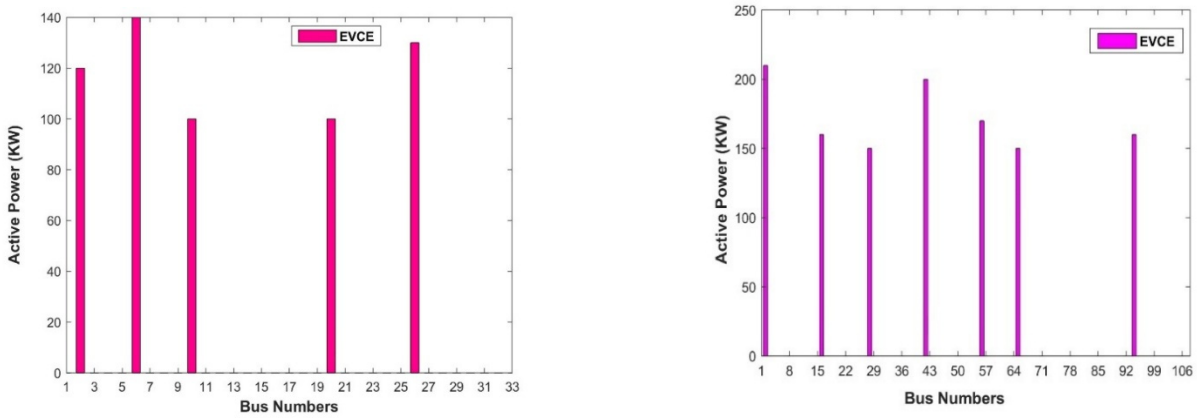

(**a**) (**b**)

Figure 1. Optimal location and size of EVCE in Case I for: (**a**) 33-bus system; and (**b**) 108-bus system.

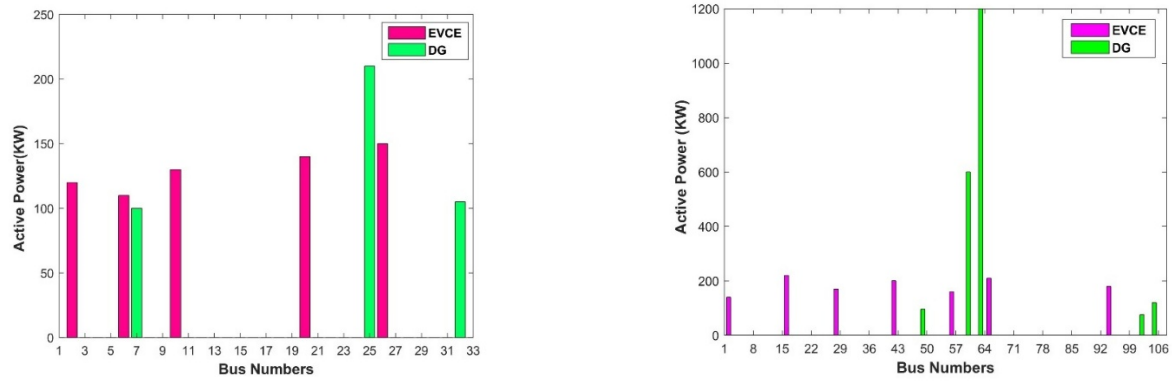

(**a**) (**b**)

Figure 2. Optimal location and size of EVCE and solar DG in Case II for: (**a**) 33-bus system; and (**b**) 108-bus system.

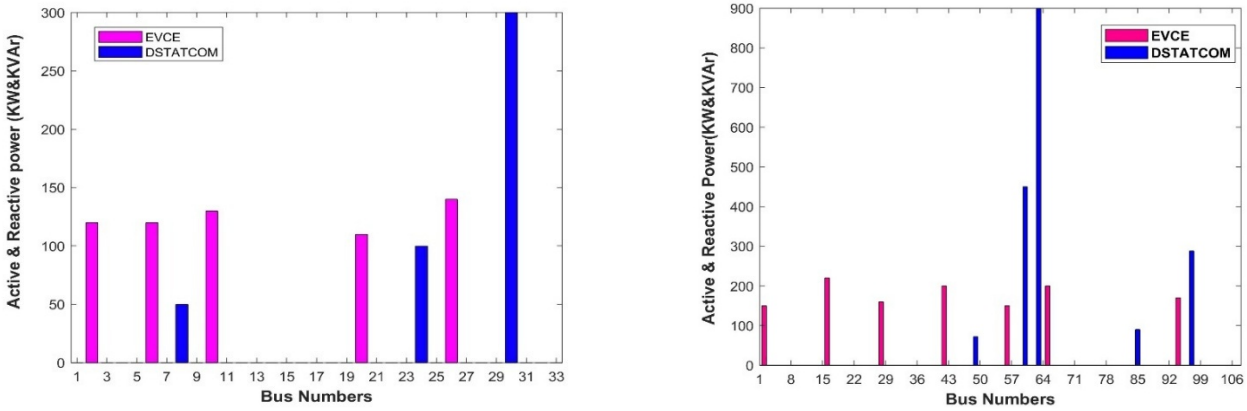

(**a**) (**b**)

Figure 3. Optimal location and size of EVCE and DSTATCOM in Case III for: (**a**) 33-bus system; and (**b**) 108-bus system.

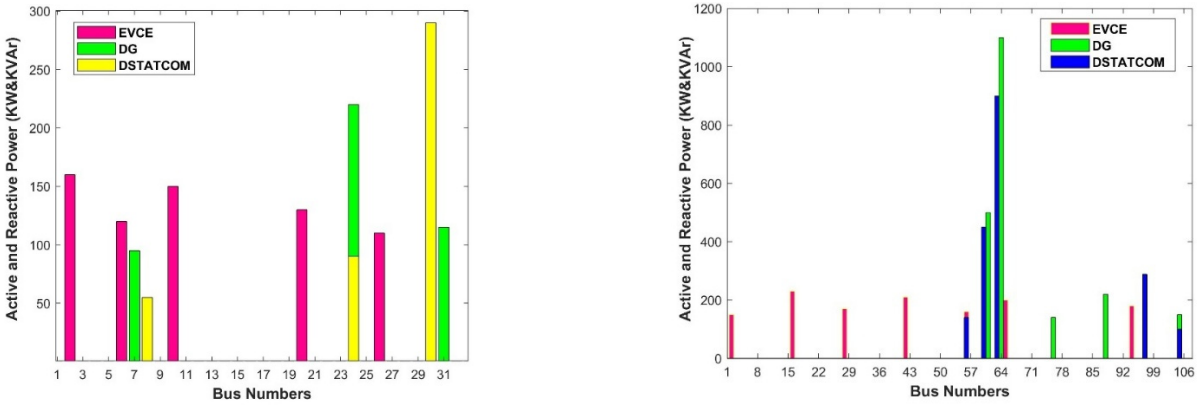

(**a**) (**b**)

Figure 4. Optimal location and size of EVCE, solar DG, and DSTATCOM in Case IV for: (**a**) 33-bus system; and (**b**) 108-bus system.

Table 2 presents the optimal EVCE capacities for both test networks in each case. The results show that in Case II, the real power provided by the solar DG boosts EV penetration by 10% and 7% for the 33-bus and 108-bus DNs, respectively, compared to Case I. In Case III, the reactive power support from the DSTATCOM increases EV penetration by 5% and

3% for the 33-bus and 108-bus DNs, respectively, in comparison to Case I. However, the highest EV penetration is observed in Case IV. This improvement is primarily due to the synergistic effect of the solar-based DG and DSTATCOM, which considerably boost the DN's ability to handle loads by supplying both active and reactive power to the system. In Case IV, for the 33-bus system, the EV penetration is increased by 12%; for the 108-bus system, penetration is increased by 9% compared to Case I, as is shown in Table 2.

Table 2. Total optimal EVCE capacity for all four cases.

	Total EVCE Capacity (kW)	
Cases	**33-Bus System**	**108-Bus System**
Case I	590	1210
Case II	650	1270
Case III	620	1250
Case IV	670	1300

(b) Results of objective functions obtained using IPSO-SR technique

The total planning cost of the proposed approach, encompassing the investment cost, energy loss cost, and emissions cost, was calculated for all cases in both the 33-bus and 108-bus systems using the IPSO-SR algorithm. The results are presented in Tables 3 and 4, corresponding to the 33-bus and 108-bus systems, respectively. From the Tables, it can be seen that Case I achieves the lowest investment cost. However, due to the absence of real and reactive power support from solar DG and DSTATCOM, respectively, it incurs the highest energy loss and emissions costs among all cases for both test systems. The presence of renewable-based DG and DSTATCOM in Case II and Case III, respectively, further increases the investment cost. However, the energy loss cost and emissions cost decrease as compared to Case I. Case IV, which incorporates the EVCE alongside high-cost components, such as DG and DSTATCOM, incurs the highest investment cost. The integration of solar-based DG and DSTATCOM together leads to a substantial decrease in both the energy loss cost and emissions cost, positioning it as the most effective and environmentally sustainable solution for both the 33-bus and 108-bus systems. From the analysis, it can be seen that the real power injection in the system increases the EVCE capacity and reduces the grid power draw, thus making the planning more sustainable by reducing the carbon emissions. On the other hand, the reactive power injection helps with respect to the renewable intermittency, enhances the voltage profile, and reduces power loss. Consequently, Case IV emerges as the most technically and economically viable solution for long-term planning from a DN operator's point of view.

Table 3. Financial analysis of all four cases for 33-bus DN.

	33-Bus Radial DN			
Cases	C_{inv} **(\$** $\times$ 10^7**)**	C_{el} **(\$** $\times$ 10^7**)**	C_{ee} **(\$** $\times$ 10^7**)**	C_{Total} **(\$** $\times$ 10^7**)**
1	3.668	1.419	0.137	5.223
2	4.136	1.234	0.125	5.495
3	3.679	1.296	0.136	5.111
4	4.335	1.049	0.123	5.509

Table 4. Financial analysis of all four cases for 108-bus DN.

108-Bus Radial DN				
Case	C_{inv} **(\$ × 10^7)**	C_{el} **(\$ × 10^7)**	C_{ee} **(\$ × 10^7)**	C_{Total} **(\$ × 10^7)**
1	7.685	2.949	0.457	11.091
2	8.108	2.586	0.409	11.108
3	7.928	2.684	0.415	11.027
4	8.537	2.321	0.378	11.235

6.3. Impact Assessment

To highlight the benefits of the proposed planning approach, a comparative analysis of all planning cases was conducted, focusing on their impact on the voltage profile, power losses, and environmental sustainability.

(a) Voltage Profile Improvement

Figure 5a and Figure 5b show the voltage profiles of all the cases for the 33-bus and 108-bus systems, respectively. In the base case, the minimum bus voltage is observed to be 0.9131 p.u. at bus 18 and 0.9224 p.u. at bus number 105 for the 33-bus and 108-bus systems, respectively. In Case I, it can be seen that the allocation of the EVCE in the 33-bus and 108-bus systems led to a decrease in the minimum bus voltage to 0.9024 p.u. in the 33-bus system and to 0.9216 p.u. in the 108-bus system. In Case II, the EVCE integrates with solar DG, in which it can be observed that the lowest voltage of both the 33-bus and 108-bus system voltages are increased to 0.9060 p.u. at bus no 18 and 0.9247 p.u. at bus no 105. Similarly, in Case III with the EVCE integrated with the DSTATCOM, the lowest bus voltages of the 33-bus and 108-bus DNs increased to 0.9082 p.u. and 0.9266 p.u., respectively. In Case IV, for the 33-bus and 108-bus DN, the lowest bus voltages increased to 0.9099 p.u. and 0.9293 p.u., respectively. Therefore, it can be concluded that Case IV yields the most favorable outcome regarding the voltage profile.

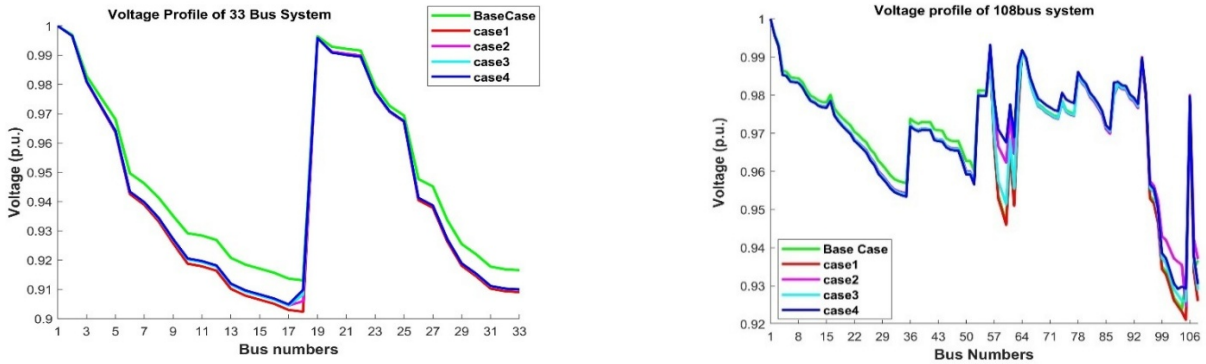

(**a**) (**b**)

Figure 5. Voltage profile of: (**a**) 33-bus system; and (**b**) 108-bus real Indian DN for all cases.

(b) Power loss

The power losses for all planning cases in both test systems are shown in Figure 6a and Figure 6b, respectively. Additionally, to provide a clearer understanding of the technical aspects of power system losses, the line losses for the 33-bus and 108-bus systems are detailed in Figure 7a,b for all cases. From the Figure, it can be seen that, due to the presence of the solar DG in Case II, the power loss is reduced in comparison to that of Case I. The presence of the DSTATCOM in Case III also decreases the power losses as compared to Case

I; however, the reduction in power loss is greater in the solar DG application than in the DSTATCOM application alone. The most significant reduction in power losses is observed in Case IV, which is attributed to the combined real and reactive power support provided by the solar DG and DSTATCOM, respectively, compared to the other planning cases.

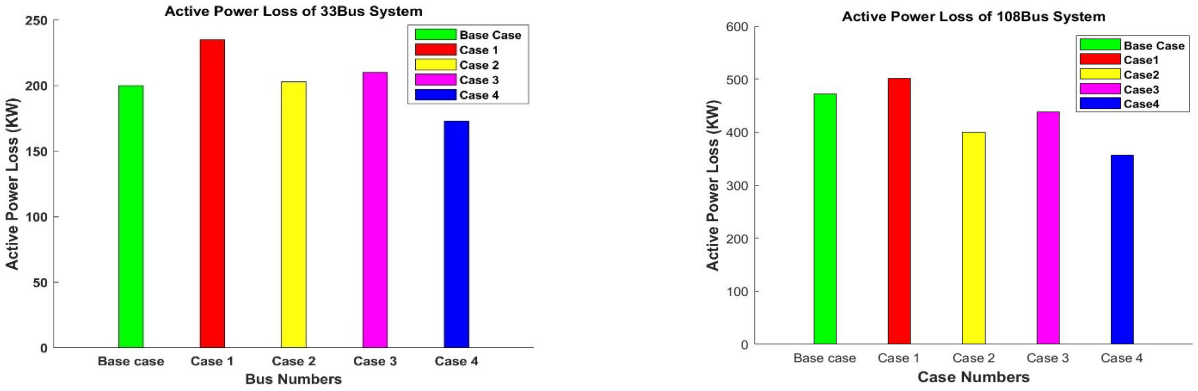

(**a**) (**b**)

Figure 6. Power losses of: (**a**) 33-bus system; and (**b**) 108-bus real Indian DN for all cases.

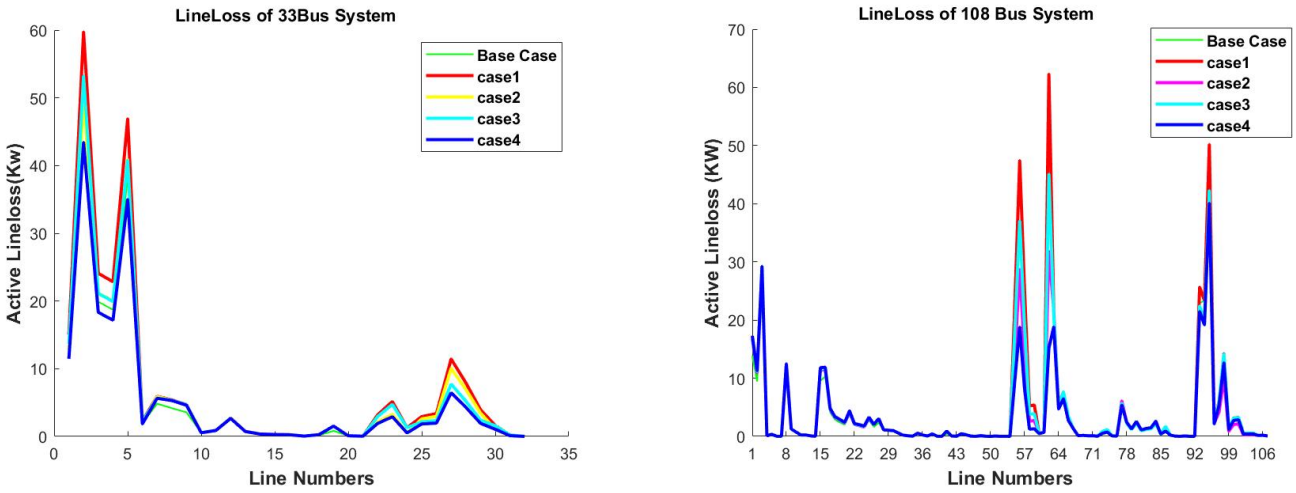

(**a**) (**b**)

Figure 7. Line losses of: (**a**) 33-bus system; and (**b**) 108-bus real Indian DN for all cases.

(c) Environmental emissions

Table 5 depicts the comparative results of total carbon emissions across all cases for both test systems over 10 years of planning. As can be seen in Table 5, in Case I, the entire demand for the EVCE is met solely by the grid, resulting in a substantial increase in carbon emissions compared to that of other cases. In contrast, the carbon emissions decrease in Case II and Case III as compared to Case I because of the presence of the solar DG and DSTATCOM, respectively. The maximum reduction in carbon emissions can be observed in Case IV due to the support of both real and reactive power, as shown in Table 5. Therefore, the maximum societal benefit occurs in Case IV.

Table 5. Grid power and CG of 33-bus and 108-bus DN.

Cases	Total Carbon Emissions (Kg × 10^7)	Cases	Total Carbon Emissions (Kg × 10^7)
1	36.81	1	121.33
2	33.24	2	108.73
3	36.02	3	112.14
4	32.17	4	100.44

The solar DG provided real power to support the grid, reducing the grid dependency and therefore providing a sustainable solution. On the other hand, the DSTATCOM helped to mitigate the low voltage profile, poor voltage stability, voltage regulation, and power losses and also helped to maintain the power factor by injecting reactive power into the system. Therefore, the study demonstrates that the integration of both the solar DG and DSTATCOM within the system yields the maximum techno–economic and environmental benefits for both the 33-bus and 108-bus DNs.

6.4. Algorithm Comparison

The performance of the proposed planning model was evaluated by comparing the IPSO-SR algorithm with other optimization techniques such as the flower pollination algorithm (FPA) [5], PSO [3], and genetic algorithm (GA) [13]. For the genetic algorithm, the crossover and mutation probabilities were set at 0.85 and 0.01, respectively. In the PSO, the accelerating factors were chosen as c1 = 0 and c2 = 2, with the inertial weight factors set to w1 = 0.45 and w2 = 0.95. In the case of the FPA, the probability switch was set at 0.85. Figure 8 presents a comparison of the convergence behavior of all the algorithms. The results clearly show that the IPSO-SR method achieves faster convergence than the other techniques.

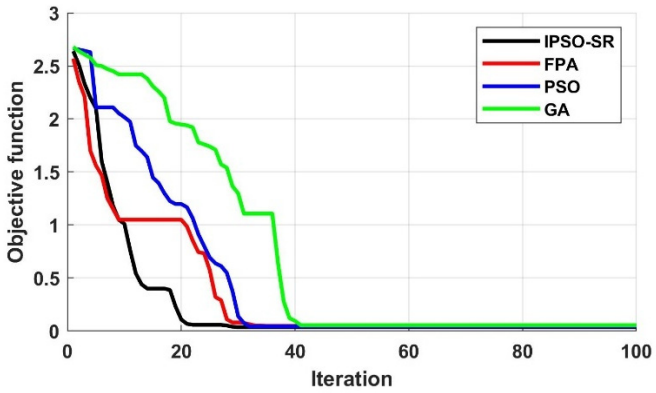

Figure 8. Comparison of convergence characteristics between different algorithms.

7. Conclusions

This study presents an innovative planning approach for DN that integrates an EVCE, DG, and DSTATCOM, focusing on technical, economic, and environmental considerations. The study determined the optimal location and size of the EVCE, DG and DSTATCOM while minimizing the costs related to installation, operations, energy losses, and emissions by employing the IPSO-SR method while adhering to system security constraints. To evaluate the long-term practicality of the proposed framework, the analysis considered key practical economic parameters, including the interest rate and inflation rate. These parameters were incorporated into the planning process to account for their impact on costs over the system's lifecycle, ensuring that the framework remains economically viable

and realistic under varying financial conditions. To further demonstrate the sustainability of the proposed configuration, an in-depth analysis of carbon emissions was conducted over a long-term planning horizon. This evaluation quantified the environmental impact of the framework by assessing the reduction in emissions achieved through the integration of the EVCE, solar DG, and DSTATCOM. By incorporating emissions factors into the analysis, the study highlights the potential of the proposed framework to support environmentally friendly energy solutions and contribute to achieving long-term sustainability goals.

The proposed methodology was validated using a 33-bus and 108-bus real Indian DN. To assist power system planning engineers in selecting the optimal planning strategy, several case studies were conducted based on different configurations of the EVCE, solar DG, and DSTATCOM, with results analyzed over a 10-year planning period. The analysis showed that the combined integration of solar DG and DSTATCOM in the DN increased the EV penetration level by 12% and 9% compared to Case I for the 33-bus and 108-bus systems, respectively. The technical analysis showed that both real and reactive power support from the DG and DSTATCOM significantly improve the voltage profile in Case IV, outperforming other configurations. Additionally, in Case IV, power losses are reduced by 36% in the 33-bus system and 40% in the 108-bus system, compared to Case I. From a financial perspective, while the investment cost increases due to the inclusion of expensive devices, energy loss costs and emissions costs are significantly reduced. Specifically, for the 33-bus system, energy loss costs and emissions costs are reduced by 35% and 27%, respectively, when both a solar DG and DSTATCOM are integrated into the system. Similarly, for the 108-bus system, the reduction in energy loss costs and emissions costs is 15% and 20%, respectively. Additionally, the environmental assessment indicated that the present planning approach results in a 14% decrease in carbon production for the 33-bus DN and a 20% reduction for the 108-bus DN.

In conclusion, it can be inferred that integrating a solar DG and DSTATCOM into the long-term planning of an EVCE is the most advantageous option from the perspective of the distribution network operator. To validate the effectiveness of the IPSO-SR technique, a comparative assessment was performed against other algorithms such as FPA, PSO, and GA. The results indicate that the IPSO-SR outperforms the other methods in terms of the convergence rate when solving the proposed planning problem.

Author Contributions: Conceptualization, R.B., S.R.G., S.C.S., S.N., S.S., and P.A.; methodology, R.B., S.R.G., S.C.S., and S.N.; software, R.B., and S.N.; validation, R.B., S.R.G., S.C.S., F.L., S.N., S.S., and P.A.; formal analysis, R.B., S.R.G., S.C.S., F.L., S.N., S.S., and P.A.; writing—original draft preparation, R.B., S.N., and S.R.G.; writing—review and editing, S.R.G., S.C.S., F.L., S.S., and P.A.; supervision, S.R.G., S.C.S., F.L., S.S., and P.A.; investigation, R.B., S.R.G., S.C.S., F.L., S.N., S.S., and P.A. All authors have read and agreed to the published version of the manuscript.

Funding: This research received no external funding.

Data Availability Statement: The datasets employed in this research, specifically for the 33-bus DN and the 108-bus Indian DN, are available in Refs. [3,37].

Acknowledgments: We sincerely thank the School of Electrical Engineering, KIIT, deemed to be the University of Bhubaneswar, for their steadfast support and motivation throughout the course of this study.

Conflicts of Interest: The authors declare no conflict of interest.

Appendix A. Bus Data and Line Data of 33-Bus DN and 108-Bus Real Indian Real DN

Table A1. Line data and bus data of 33-bus distribution system.

Branch Number	Sending End Bus	Receiving End Bus	Active Power (MW)	Reactive Power (MVAr)	Resistance (Ω)	Reactance (Ω)
1	1	2	0.0922	0.047	0	0
2	2	3	0.493	0.2511	0.1	0.06
3	3	4	0.366	0.1864	0.09	0.04
4	4	5	0.3811	0.1941	0.12	0.08
5	5	6	0.819	0.707	0.06	0.03
6	6	7	0.1872	0.6188	0.06	0.02
7	7	8	0.7114	0.2351	0.2	0.01
8	8	9	1.03	0.74	0.2	0.01
9	9	10	1.044	0.74	0.06	0.02
10	10	11	0.1966	0.065	0.06	0.02
11	11	12	0.3744	0.1238	0.045	0.03
12	12	13	1.468	1.155	0.06	0.035
13	13	14	0.5416	0.7129	0.06	0.035
14	14	15	0.591	0.526	0.12	0.08
15	15	16	0.7463	0.545	0.06	0.01
16	16	17	1.289	1.721	0.06	0.02
17	17	18	0.732	0.574	0.06	0.02
18	2	19	0.164	0.1565	0.09	0.04
19	19	20	1.5042	1.3554	0.09	0.04
20	20	21	0.4095	0.4784	0.09	0.04
21	21	22	0.7089	0.9373	0.09	0.04
22	3	23	0.4512	0.3083	0.09	0.04
23	23	24	0.898	0.7091	0.09	0.05
24	24	25	0.896	0.7011	0.42	0.2
25	6	26	0.203	0.1034	0.42	0.2
26	26	27	0.2842	0.1447	0.06	0.025
27	27	28	1.059	0.9337	0.06	0.025
28	28	29	0.8042	0.7006	0.06	0.02
29	29	30	0.5075	0.2585	0.12	0.07
30	30	31	0.9744	0.963	0.2	0.06
31	31	32	0.3105	0.3619	0.15	0.07
32	32	33	0.341	0.5302	0.21	0.1
33	21	8	2	2	0.06	0.04

Table A2. Line data and bus data for real Indian 108-bus distribution system.

Branch Number	Sending End Bus	Receiving End Bus	Active Power (MW)	Reactive Power (MVAr)	Resistance (Ω)	Reactance (Ω)
1	1	2	0.0814	0.0921	0	0
2	2	3	0.0555	0.0628	0	0
3	3	4	0.1443	0.1632	0	0
4	4	5	0.2970	0.0470	0	0
5	5	6	1.1550	0.1827	96	72
6	6	7	0.2970	0.0470	38.4	28.8
7	7	8	0.5940	0.0940	38.4	28.8
8	4	9	0.0666	0.0753	60	45
9	9	10	0.5940	0.0940	0	0
10	10	11	0.6270	0.0992	60	45
11	11	12	0.2970	0.0470	60	45

Table A2. *Cont.*

Branch Number	Sending End Bus	Receiving End Bus	Active Power (MW)	Reactive Power (MVAr)	Resistance (Ω)	Reactance (Ω)
12	12	13	0.4950	0.0783	60	45
13	13	14	0.2970	0.0470	98.4	73.8
14	14	15	0.2970	0.0470	60	45
15	9	16	0.0814	0.0921	96	72
16	16	17	0.0925	0.1046	96	72
17	17	18	0.0396	0.0385	96	72
18	18	19	0.0352	0.0342	96	72
19	19	20	0.0396	0.0385	96	72
20	20	21	0.0352	0.0342	96	72
21	21	22	0.0999	0.0424	96	72
22	22	23	0.0555	0.0236	96	72
23	23	24	0.0888	0.0377	96	72
24	24	25	0.0888	0.0377	0	0
25	25	26	0.1665	0.0707	96	72
26	26	27	0.1650	0.0261	96	72
27	27	28	0.2970	0.0470	96	72
28	28	29	0.2310	0.0365	96	72
29	29	30	0.2970	0.0470	0	0
30	30	31	0.3960	0.0626	96	72
31	31	32	0.3630	0.0574	96	72
32	32	33	0.2310	0.0365	96	72
33	33	34	0.2640	0.0418	96	72
34	34	35	0.3630	0.0574	96	72
35	18	36	0.6270	0.0992	96	72
36	36	37	0.6270	0.0992	96	72
37	37	38	0.6270	0.0992	96	72
38	19	39	0.4950	0.0783	96	72
39	39	40	0.1980	0.0313	96	72
40	39	41	0.2310	0.0365	96	72
41	21	42	0.4950	0.0783	96	72
42	42	43	0.1650	0.0261	96	72
43	43	44	0.1650	0.0261	96	72
44	23	45	0.2970	0.0470	96	72
45	45	46	0.2970	0.0470	96	72
46	46	47	0.2970	0.0470	96	72
47	46	48	0.2310	0.0365	96	72
48	26	49	0.2970	0.0470	192	144
49	28	50	0.1980	0.0313	96	72
50	50	51	0.3630	0.0574	0	0
51	30	52	0.4950	0.0783	96	72
52	10	53	0.2970	0.0470	60	45
53	10	54	0.5940	0.0940	60	45
54	54	55	0.2970	0.0470	0	0
55	1	56	0.6660	0.2826	0	0
56	56	57	1.5540	0.6594	0	0
57	57	58	1.1100	0.4710	0	0
58	58	59	0.3330	0.1413	0	0
59	59	60	0.3441	0.1460	1200	900
60	57	61	0.8250	0.1305	240	180
61	58	62	1.1550	0.1827	240	180
62	1	63	1.0560	0.7128	2400	1800
63	1	64	0.3960	0.2673	0	0
64	64	65	0.0990	0.0668	0	0
65	65	66	0.8580	0.1357	240	180
66	66	67	0.6930	0.1096	0	0
67	67	68	1.0230	0.1618	240	180
68	68	69	0.8910	0.1409	0	0
69	69	70	1.1550	0.1827	0	0

Table A2. *Cont.*

Branch Number	Sending End Bus	Receiving End Bus	Active Power (MW)	Reactive Power (MVAr)	Resistance (Ω)	Reactance (Ω)
70	70	71	0.6930	0.1096	0	0
71	71	72	0.7590	0.1201	60	45
72	72	73	0.6600	0.1044	60	45
73	67	74	0.7260	0.1148	0	0
74	74	75	1.0230	0.1618	240	180
75	75	76	0.8910	0.1409	0	0
76	76	77	0.4950	0.0783	96	72
77	65	78	0.3663	0.1554	0	0
78	78	79	0.2220	0.0942	0	0
79	79	80	0.1980	0.0313	0	0
80	80	81	0.4620	0.0731	0	0
81	81	82	0.2640	0.0418	0	0
82	82	83	0.3630	0.0574	0	0
83	83	84	0.4950	0.0783	60	45
84	84	85	1.0890	0.1723	240	180
85	85	86	0.6600	0.1044	240	180
86	78	87	2.9700	0.4698	240	180
87	79	88	0.3630	0.0574	240	180
88	80	89	0.9240	0.1462	0	0
89	89	90	0.4620	0.0731	60	45
90	81	91	0.6270	0.0992	96	72
91	82	92	0.1650	0.0261	38.4	28.8
92	83	93	0.2310	0.0365	60	45
93	1	94	0.6549	0.2779	0	0
94	94	95	0.6660	0.2826	0	0
95	95	96	1.8870	0.8007	0	0
96	96	97	0.0999	0.0424	768	576
97	97	98	0.8580	0.1357	0	0
98	98	99	2.0460	0.3236	0	0
99	99	100	0.2970	0.0470	0	0
100	100	101	0.6930	0.1096	0	0
101	101	102	0.7260	0.1148	151.2	113.4
102	102	103	0.8250	0.1305	0	0
103	103	104	0.8250	0.1305	0	0
104	104	105	0.8580	0.1357	240	180
105	95	106	0.2970	0.0470	240	180
106	99	107	0.7260	0.1148	151.2	113.4
107	102	108	0.0990	0.0157	240	180

References

1. Chen, T.; Zhang, X.-P.; Wang, J.; Li, J.; Wu, C.; Hu, M.; Bian, H. A Review on Electric Vehicle Charging Infrastructure Development in the UK. *J. Mod. Power Syst. Clean Energy* **2020**, *8*, 193–205. [CrossRef]
2. Deb, S.; Tammi, K.; Kalita, K.; Mahanta, P. Impact of Electric Vehicle Charging Station Load on Distribution Network. *Energies* **2018**, *11*, 178. [CrossRef]
3. Nandi, S.; Ghatak, S.R.; Acharjee, P. Multi-Scenario Based Optimal Planning of Distribution Network Considering Fast Electric Vehicle Charging Station. In Proceedings of the 2024 IEEE 4th International Conference on Sustainable Energy and Future Electric Transportation (SEFET), Hyderabad, India, 31 July–3 August 2024; pp. 1–6.
4. Agrawal, S.; Soni, R. Renewable Energy: Sources, Importance and Prospects for Sustainable Future. In *Energy*; Singh, P., Singh, S., Kumar, G., Baweja, P., Eds.; Wiley: Hoboken, NJ, USA, 2021; pp. 131–150. ISBN 978-1-119-74144-2.
5. Nandi, S.; Ghatak, S.R.; Sannigrahi, S.; Acharjee, P. Coordinated Planning and Operation of PV- Hydrogen Integrated Distribution Network Incorporating Daily-Seasonal Green Hydrogen Storage and EV Charging Station. *Int. J. Hydrogen Energy* **2024**, *90*, 134–158. [CrossRef]
6. He, H.; Lu, Z.; Guo, X.; Shi, C.; Jia, D.; Chen, C.; Guerrero, J. Optimized Control Strategy for Photovoltaic Hydrogen Generation System with Particle Swarm Algorithm. *Energies* **2022**, *15*, 1472. [CrossRef]
7. Ferminus Raj, A.; Gnana Saravanan, A. An Optimization Approach for Optimal Location & Size of DSTATCOM and DG. *Appl. Energy* **2023**, *336*, 120797. [CrossRef]

8. Sayed, M.A.; Atallah, R.; Assi, C.; Debbabi, M. Electric Vehicle Attack Impact on Power Grid Operation. *Int. J. Electr. Power Energy Syst.* **2022**, *137*, 107784. [CrossRef]
9. Kanojia, S.; Suthar, B.N. Voltage Stability Analysis in Modern Power System Considering Wind Energy Conversion System. In Proceedings of the 2023 IEEE IAS Global Conference on Emerging Technologies (GlobConET), London, UK, 19–21 May 2023; pp. 1–7.
10. Liang, X.; Chai, H.; Ravishankar, J. Analytical Methods of Voltage Stability in Renewable Dominated Power Systems: A Review. *Electricity* **2022**, *3*, 75–107. [CrossRef]
11. Ghatak, S.R.; Basu, D.; Acharjee, P. Voltage Profile Improvement and Loss Reduction Using Optimal Allocation of SVC. In Proceedings of the 2015 Annual IEEE India Conference (INDICON), New Delhi, India, 17–20 December 2015; pp. 1–6.
12. Paredes, L.A.; Molina, M.G.; Serrano, B.R. Enhancing Dynamic Voltage Stability in Resilient Microgrids Using FACTS Devices. *IEEE Access* **2023**, *11*, 66150–66176. [CrossRef]
13. Pagidipala, S.; Sandeep, V. Optimal Planning of Electric Vehicle Charging Stations and Distributed Generators with Network Reconfiguration in Smart Distribution Networks Considering Uncertainties. *Meas. Sens.* **2024**, *36*, 101400. [CrossRef]
14. Yuvaraj, T.; Suresh, T.D.; Meyyappan, U.; Aljafari, B.; Thanikanti, S.B. Optimizing the Allocation of Renewable DGs, DSTATCOM, and BESS to Mitigate the Impact of Electric Vehicle Charging Stations on Radial Distribution Systems. *Heliyon* **2023**, *9*, e23017. [CrossRef]
15. Tiwari, D.; Ghatak, S.R. Performance Enhancement of Distribution System Using Optimal Allocation of Distributed Generation & DSTATCOM. In Proceedings of the 2017 International Conference on Innovative Mechanisms for Industry Applications (ICIMIA), Bengaluru, India, 21–23 February 2017; pp. 533–538.
16. Roy Ghatak, S.; Sannigrahi, S.; Acharjee, P. Comparative Performance Analysis of DG and DSTATCOM Using Improved PSO Based on Success Rate for Deregulated Environment. *IEEE Syst. J.* **2018**, *12*, 2791–2802. [CrossRef]
17. Mohanty, A.K.; Babu, P.S.; Salkuti, S.R. Fuzzy-Based Simultaneous Optimal Placement of Electric Vehicle Charging Stations, Distributed Generators, and DSTATCOM in a Distribution System. *Energies* **2022**, *15*, 8702. [CrossRef]
18. B. C., S.; A., U.; R. S., G. Optimal Planning of PV Sources and D-STATCOM Devices with Network Reconfiguration Employing Modified Ant Lion Optimizer. *Energies* **2024**, *17*, 2238. [CrossRef]
19. Sannigrahi, S.; Ghatak, S.R.; Basu, D.; Acharjee, P. Optimal Placement of DSTATCOM, DG and Their Performance Analysis in Deregulated Power System. *Int. J. Power Energy Convers.* **2019**, *10*, 105. [CrossRef]
20. Jin, Y.; Acquah, M.A.; Seo, M.; Han, S. Optimal Siting and Sizing of EV Charging Station Using Stochastic Power Flow Analysis for Voltage Stability. *IEEE Trans. Transp. Electrif.* **2023**, *10*, 777–794. [CrossRef]
21. Krishnamurthy, N.K.; Sabhahit, J.N.; Jadoun, V.K.; Gaonkar, D.N.; Shrivastava, A.; Rao, V.S.; Kudva, G. Optimal Placement and Sizing of Electric Vehicle Charging Infrastructure in a Grid-Tied DC Microgrid Using Modified TLBO Method. *Energies* **2023**, *16*, 1781. [CrossRef]
22. Sengor, I.; Erenoglu, A.K.; Guldorum, H.C.; Erdinc, O.; Taşcıkaraoğlu, A.; Taştan, İ.C.; Büyük, A.F.; Catalão, J.P.S. Optimal Sizing and Siting of Different Types of EV Charging Stations in a Real Distribution System Environment. *IET Renew. Power Gener.* **2022**, *16*, 3171–3183. [CrossRef]
23. Chen, L.; Xu, C.; Song, H.; Jermsittiparsert, K. Optimal Sizing and Sitting of EVCS in the Distribution System Using Metaheuristics: A Case Study. *Energy Rep.* **2021**, *7*, 208–217. [CrossRef]
24. Pal, A.; Bhattacharya, A.; Chakraborty, A.K. Allocation of EV Fast Charging Station with V2G Facility in Distribution Network. In Proceedings of the 2019 8th International Conference on Power Systems (ICPS), Jaipur, India, 20–22 December 2019; pp. 1–6.
25. Jamatia, P.; Bhattacharjee, S.; Sharma, S. Optimal Allocation of EV Charging Station in Distribution Network. In Proceedings of the 2022 4th International Conference on Energy, Power and Environment (ICEPE), Shillong, India, 29 April–1 May 2022; pp. 1–6.
26. Karmaker, A.K.; Hossain, M.A.; Pota, H.R.; Onen, A.; Jung, J. Energy Management System for Hybrid Renewable Energy-Based Electric Vehicle Charging Station. *IEEE Access* **2023**, *11*, 27793–27805. [CrossRef]
27. Kumar, N.; Kumar, T.; Nema, S.; Thakur, T. A Comprehensive Planning Framework for Electric Vehicles Fast Charging Station Assisted by Solar and Battery Based on Queueing Theory and Non-Dominated Sorting Genetic Algorithm-II in a Co-Ordinated Transportation and Power Network. *J. Energy Storage* **2022**, *49*, 104180. [CrossRef]
28. Ahmad, F.; Iqbal, A.; Asharf, I.; Marzband, M.; Khan, I. Placement and Capacity of EV Charging Stations by Considering Uncertainties With Energy Management Strategies. *IEEE Trans. Ind. Appl.* **2023**, *59*, 3865–3874. [CrossRef]
29. El-Ela, A.A.A.; Mouwafi, M.T.; Elbaset, A.A. Optimal Combination of DGs and Capacitor Banks for Performance Enhancement of Distribution Systems. In *Modern Optimization Techniques for Smart Grids*; Springer International Publishing: Cham, Switzerland, 2023; pp. 141–176. ISBN 978-3-030-96024-7.
30. Ćetković, D.; Komen, V. Optimal Distributed Generation and Capacitor Bank Allocation and Sizing at Two Voltage Levels. *IEEE Syst. J.* **2023**, *17*, 5831–5841. [CrossRef]
31. Pal, A.; Bhattacharya, A.; Chakraborty, A.K. Planning of EV Charging Station With Distribution Network Expansion Considering Traffic Congestion and Uncertainties. *IEEE Trans. Ind. Appl.* **2023**, *59*, 3810–3825. [CrossRef]

32. Yuvaraj, T.; Devabalaji, K.R.; Thanikanti, S.B.; Aljafari, B.; Nwulu, N. Minimizing the Electric Vehicle Charging Stations Impact in the Distribution Networks by Simultaneous Allocation of DG and DSTATCOM with Considering Uncertainty in Load. *Energy Rep.* **2023**, *10*, 1796–1817. [CrossRef]
33. Saw, B.K.; Bohre, A.K.; Jobanputra, J.H.; Kolhe, M.L. Solar-DG and DSTATCOM Concurrent Planning in Reconfigured Distribution System Using APSO and GWO-PSO Based on Novel Objective Function. *Energies* **2022**, *16*, 263. [CrossRef]
34. Mahdad, B. Towards Sustainable Integration of STATCOM and DGs Based Radial Distribution Systems Using Dynamic Adaptive Aquila Optimizer. *Process Integr. Optim. Sustain.* **2023**, *7*, 381–405. [CrossRef]
35. Montoya, O.D.; Molina-Cabrera, A.; Giral-Ramírez, D.A.; Rivas-Trujillo, E.; Alarcón-Villamil, J.A. Optimal Integration of D-STATCOM in Distribution Grids for Annual Operating Costs Reduction via the Discrete Version Sine-Cosine Algorithm. *Results Eng.* **2022**, *16*, 100768. [CrossRef]
36. Sen, D.; Ghatak, S.R.; Acharjee, P. Optimal Allocation of Static VAR Compensator by a Hybrid Algorithm. *Energy Syst.* **2019**, *10*, 677–719. [CrossRef]
37. Nandi, S.; Ghatak, S.R.; Acharjee, P.; Lopes, F. Multi-Scenario-Based Strategic Deployment of Electric Vehicle Ultra-Fast Charging Stations in a Radial Distribution Network. *Energies* **2024**, *17*, 4204. [CrossRef]
38. Dolatabadi, S.H.; Ghorbanian, M.; Siano, P.; Hatziargyriou, N.D. An Enhanced IEEE 33 Bus Benchmark Test System for Distribution System Studies. *IEEE Trans. Power Syst.* **2021**, *36*, 2565–2572. [CrossRef]
39. Meena, N.K.; Swarnkar, A.; Gupta, N.; Niazi, K.R. Optimal Integration of DERs in Coordination with Existing VRs in Distribution Networks. *IET Gener. Transm. Distrib.* **2018**, *12*, 2520–2529. [CrossRef]
40. Gupta, R.S.; Anand, Y.; Tyagi, A.; Anand, S. Sustainable Charging Station Allocation in the Distribution System for Electric Vehicles Considering Technical, Economic, and Societal Factors. *J. Energy Storage* **2023**, *73*, 109052. [CrossRef]
41. Roy Ghatak, S.; Sannigrahi, S.; Acharjee, P. Optimised Planning of Distribution Network with Photovoltaic System, Battery Storage, and DSTATCOM. *IET Renew. Power Gener.* **2018**, *12*, 1823–1832. [CrossRef]

Disclaimer/Publisher's Note: The statements, opinions and data contained in all publications are solely those of the individual author(s) and contributor(s) and not of MDPI and/or the editor(s). MDPI and/or the editor(s) disclaim responsibility for any injury to people or property resulting from any ideas, methods, instructions or products referred to in the content.